Edge states in a circular quantum dot

Craig S. Lent
Department of Electrical Engineering, University of Notre Dame, Notre Dame, Indiana 46556
(Received 25 July 1990; revised manuscript received 3 October 1990)

The wave functions and currents in a circular quantum dot in a perpendicular magnetic field are calculated. The current in condensed (high-field) eigenstates is composed of concentric rings of current flowing in opposite directions. The current flow near the dot center flows in the direction opposite that expected from the Lorentz force. It is this inner circulation that is responsible for the "reverse" current flow associated with edge states. The correspondence between the quantum-mechanical currents and classical-particle trajectories is examined.

I. INTRODUCTION

Under a perpendicular applied magnetic field, the unconfined states of a two-dimensional electron gas (2DEG) form infinitely degenerate Landau levels whose energy increases linearly with the applied field. The Landau-level eigenstates can be thought of as localized states corresponding to the cyclotron orbits of classical electrons. If the 2DEG is confined further in the plane by a potential barrier, the energy of the states near the boundary will be altered. Further, it has long been recognized that states near the boundary produce a current which flows in a direction opposite to the circulation of inner orbits. These edge states, and their importance as a paramagnetic correction to the Landau diamagnetism, were discussed by Darwin,[1] who considered electrons in a parabolic confining potential for which analytic solutions exist. Further investigation of the effects of the edge states was done by Dingle,[2] and more recently, by Robnik.[3]

Interest in the behavior of small systems which are confined in three dimensions has been stimulated by the fabrication of individual dots and quantum-dot arrays in semiconductors.[4–7] Kumar, Laux, and Stern have solved the Schrödinger and Poisson equations self-consistently in three dimensions to obtain the electronic states for a quantum dot in a magnetic field.[8] Maksym and Chakraborty have examined the effects of electron-electron interactions in parabolic dots.[9]

In this paper we examine the one-electron states of a circular dot in a magnetic field. We take a simpler approach than Kumar, Laux, and Stern, using a fixed potential and assuming complete confinement in the plane of the 2DEG. Attention is focused here on the currents induced by the applied field and the correspondence between the quantum-mechanical results and classical cyclotron orbits. Our aim is to establish the precise nature of edge states and their relationship to the classical "skipping" orbits. The self-consistent potential obtained by Kumar, Laux, and Stern can be approximated by a flat potential with parabolic walls. After examining the hard-wall boundary case, we consider the effect of such soft walls. The numerical approach used here is similar to that of Stikova, Smrcka, and Isihara,[10] and Weisz and Berggren.[11] The calculation is performed in the framework of a single-band effective-mass model, neglecting electron-electron interactions and ignoring spin effects. Results for the circular dot which is completely confined in the plane are applicable directly to a cylindrical quantum wire. Fabrication of such structures has been reported by Reed and co-workers.[5]

II. THEORY

We consider the bound states of a particle in a two-dimensional circular quantum dot with an applied magnetic field described by a vector potential $\mathbf{A}$. The canonical momentum is given by

$$\mathbf{P}=m^*\mathbf{V}+q\,\mathbf{A}\ . \tag{1}$$

The effective-mass Hamiltonian for such a particle bound in an axially symmetric potential V_r is

$$H=\frac{1}{2m^*}(\mathbf{P}-q\,\mathbf{A})^2+V_r\ . \tag{2}$$

A completely unconstrained 2DEG in an applied magnetic field is described by the Landau Hamiltonian H_L,

$$H_L=\frac{1}{2m^*}(\mathbf{P}-q\,\mathbf{A})^2\ . \tag{3}$$

We examine the case of a perpendicular magnetic field $\mathbf{B}=\nabla\times\mathbf{A}=B_0\hat{\mathbf{z}}$ and use the symmetric gauge for the vector potential:

$$\mathbf{A}=(-B_0y/2,B_0x/2,0)\ . \tag{4}$$

The Hamiltonian can then be written in the form

$$H=\frac{1}{2m^*}(P_x^2+P_y^2)+\frac{\omega_c}{2}L_z+\frac{m^*\omega_c^2}{8}(X^2+Y^2)+V_r\ , \tag{5}$$

where L_z is the operator associated with the z component of angular momentum

$$L_z=XP_y-YP_x\ , \tag{6}$$

and

$$\omega_c = \frac{-qB_0}{m^*} \tag{7}$$

is the cyclotron frequency defined so that an electron has a positive ω_c corresponding to a counterclockwise orbit in the plane.

The bound states of the quantum dot (for any field) can be labeled by the radial quantum number n_r and the angular quantum number m. At zero magnetic field, the Hamiltonian is symmetric under time reversal so that $E(n_r,m)=E(n_r,|m|)$. The application of the magnetic field breaks this symmetry and the energy of positive-m states increase while negative-m states are lowered. The perturbation is dominated for low fields by the term linear in the field. The resulting splitting is due to the familiar paramagnetic interaction between a magnetic dipole and the applied field. As the field increases the (diamagnetic) quadratic term in (5), due to the induced current, becomes significant. Negative-m states which initially were reduced in energy, begin to increase and combine together, undergoing a transition from paramagnetic states to diamagnetic states at a field strength which depends on m. The negative-m states which have undergone this transition combine with n_L+1 states with positive or zero m (states that are always diamagnetic) to form the degenerate Landau levels (labeled by quantum number n_L). We refer to the coalescence of these energy levels as "Landau condensation" after Robnik.[3]

III. NUMERICAL RESULTS

A. Energy levels

We begin by examining the quantum dot with infinite hard walls. The potential V_r is zero if $r<R$ and infinite otherwise. The effective-mass Schrödinger equation for the Hamiltonian given by (2) was solved numerically using the finite element method. An effective mass of $0.05m_0$ was used. The symmetric gauge given by Eq. (4) was used. The discretization was performed on a square 49×49 node mesh. Eigenfunctions and eigenvalues were calculated using the subspace iteration technique for the lowest 20 eigenstates.

Figure 1 shows the eigenvalue spectrum as a function of applied magnetic field for the first 20 eigenstates. The calculation was performed for a dot with radius $R=500$ Å. Because all of the results scale with the de Broglie wavelength of the electron, they can be represented in a dimensionless form by appropriately scaling the energies and magnetic fields. The eigenenergies are scaled to E_0, the energy of the zero-field ground state. The magnetic field is plotted as the dimensionless quantity

$$\beta = \frac{eB\pi R^2}{\pi\hbar} . \tag{8}$$

For the 500-Å dot, $\beta=35$ corresponds to 9.21 T and $E_0=1.8$ meV.

The condensation of the bound states of the dot into degenerate Landau levels is clearly evident in the figure. At every value of the applied field, n_r and m remain good quantum numbers. The components which merge to form the first three Landau levels are enumerated below:

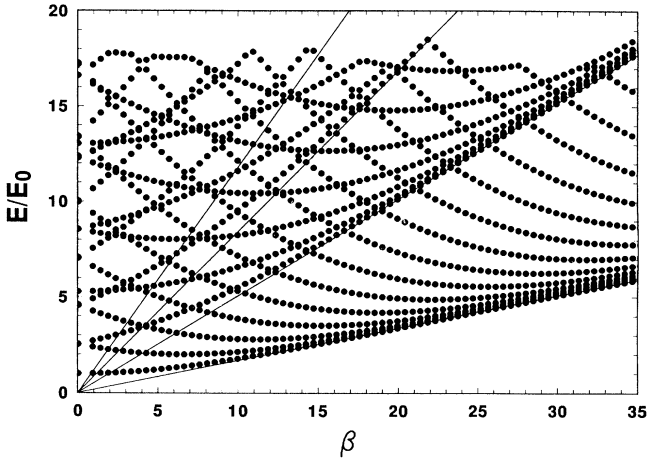

FIG. 1. Bound-state energy levels of a circular quantum dot as a function of applied magnetic field, $\beta=eB\pi R^2/\pi\hbar$. The energies are in units of E_0, the zero-field ground-state energy.

$$\begin{aligned}
&n_L=0 ,\\
&n_r=0,\quad m=0,-1,-2,\ldots,-\infty ;\\
&n_L=1,\quad n_r=0,\quad m=1 ,\\
&\qquad\quad n_r=1,\quad m=0,-1,-2,\ldots,-\infty ;\\
&n_L=2,\quad n_r=0,\quad m=2\\
&\qquad\quad n_r=1,\quad m=1\\
&\qquad\quad n_r=2,\quad m=0,-1,-2,\ldots,-\infty .
\end{aligned} \tag{9}$$

The condensation seen here does not occur in confining potentials which are parabolic. In such a potential the magnetic localization is never sufficient to isolate the electron from the walls. Parabolic potentials may be more appropriate for some dot structures examined experimentally.[12,13] Further, Demel *et al.*[13] have measured anticrossing of the energy levels in contrast to the crossing behavior in Fig. 1. They interpret these results as due to electron-electron interactions which are absent in our model.

B. Current flow

For each eigenstate, the particle (probability) current is calculated from the computed wave functions $\psi(x,y)$, using the relations,

$$\mathbf{j}=\mathbf{j}_0+\mathbf{j}_A , \tag{10}$$

$$\mathbf{j}_0=\frac{i\hbar}{2m^*}(\psi\nabla\psi^*-\psi^*\nabla\psi) , \tag{11}$$

$$\mathbf{j}_A=\frac{1}{m^*}e\,\mathbf{A}|\psi|^2 . \tag{12}$$

These relations are for electrons and the symbol e

represents the magnitude of the electronic charge. Writing the current this way separates the contribution of the wave function from that of the vector potential. This division, though gauge dependent, is helpful in understanding the nature of the eigenstates.

Figures 2–6 show the calculated current density in the dot and the probability density $|\psi|^2$ across the dot center for several eigenstates at a field of $B=5$ T ($\beta=19$). Figures 2 and 3 show the current for the $m=0$ and $m=-2$ states of the first Landau level. At this field, these states have already condensed (i.e., become degenerate with other states at the energy of a Landau level). Figure 4 shows the uncondensed $m=-7$, $n_L=0$ level. The uncondensed $n_L=1$, $m=0$, and $m=-3$ states are shown in Figs. 5 and 6.

The current flows depicted in the figures are not all easily explained by appealing to the usual classical-orbit notions. The condensed $m=0$ state shown in Fig. 2 corresponds to the classical picture of counterclockwise orbit caused by the Lorenz force on the electron. The negative-m state shown in Fig. 3 is somewhat more surprising. Rather than a central, counterclockwise current, we see a clockwise circulation in the center, surrounded by a counterclockwise outer current. This is characteristic of all the condensed negative-m states. The literature has frequently invoked the concept of "edge states" which corresponds to classical orbits that skip along the perimeter and thus carry the (particle) current clockwise, opposite that of the counterclockwise current induced in the bulklike central region. One might expect to see these edge states characterized by a clockwise current in the perimeter (edge) region of the dot. The $n_L=0$, $m=-7$ state depicted in Fig. 4 corresponds to this idea. The uncondensed $n_L=1$, $m=-3$ state in Fig. 6 should also be an edge state. Yet it has a weak perimeter current which is counterclockwise (bulklike) and an interior current which is clockwise. Below, we examine the quantum-mechanical argument for these, at first surprising, current-flow patterns. We then discuss the correspondence between the quantum wave functions and the classical orbits.

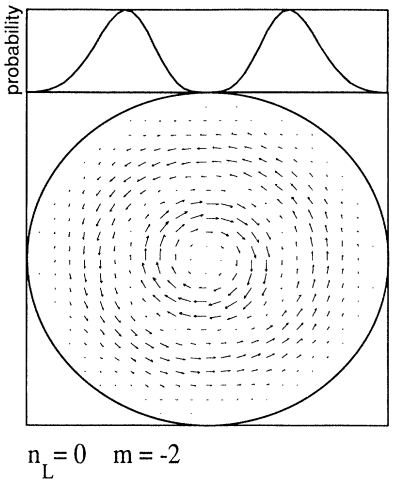

FIG. 3. Probability currents for the $n_L=0$, $m=-2$ eigenstate of a circular quantum dot. The magnetic field corresponds to $\beta=19.0$. The probability density across the dot center is shown in the upper portion of the figure.

The current $\mathbf{j}_0$ can be written in terms of ϕ, the complex phase of the wave function, and the probability density $n(\mathbf{r})=|\psi|^2$,

$$\mathbf{j}_0(\mathbf{r})=\frac{n(\mathbf{r})}{m^*}\hbar\nabla\phi(\mathbf{r}) \ . \tag{13}$$

Since each eigenstate of H is an eigenstate of L_z with ei-

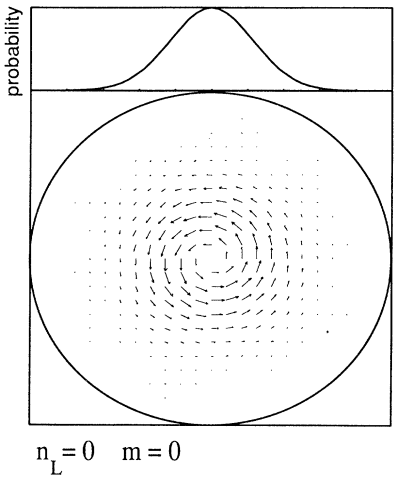

FIG. 2. Probability currents for the $n_L=0$, $m=0$ eigenstate of a circular quantum dot. The magnetic field corresponds to $\beta=19.0$ ($B=5$ T for a dot with 500-Å radius). The probability density across the dot center is shown in the upper portion of the figure.

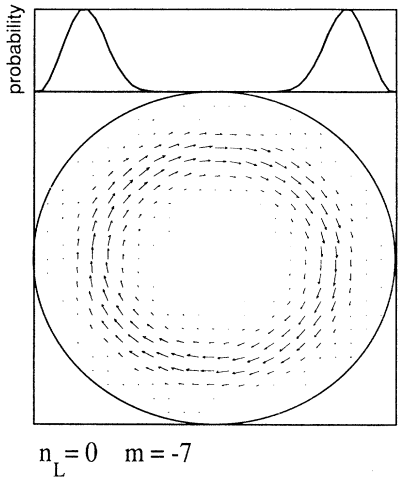

FIG. 4. Probability currents for the $n_L=0$, $m=-7$ eigenstate of a circular quantum dot. The magnetic field corresponds to $\beta=19.0$. The probability density across the dot center is shown in the upper portion of the figure.

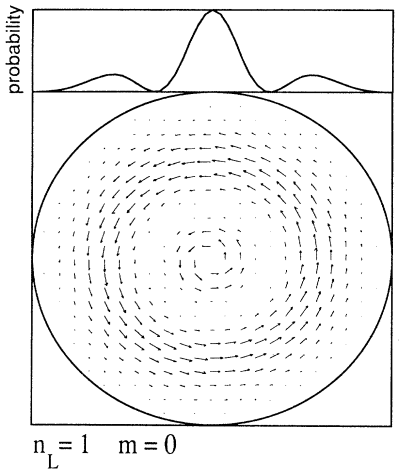

FIG. 5. Probability currents for the $n_L=1$, $m=0$ eigenstate of a circular quantum dot. The magnetic field corresponds to $\beta=19.0$. The probability density across the dot center is shown in the upper portion of the figure.

genvalue $m\hbar$, we can write the complex phase in polar coordinates as $\phi(r,\theta)=m\theta$. Therefore,

$$\mathbf{j}_0(r)=\frac{n(r)}{m^*}\hbar m\hat{\theta}\ , \tag{14}$$

where $\hat{\theta}$ is the unit vector in the θ direction. The zero-field current of the eigenstate is simply a circulation around the origin which is proportional to the angular momentum. In polar coordinates, the explicitly field-dependent part of the current can be written,

$$\mathbf{j}_A(r)=\frac{n(r)}{2m^*}eB_0r\hat{\theta}\ . \tag{15}$$

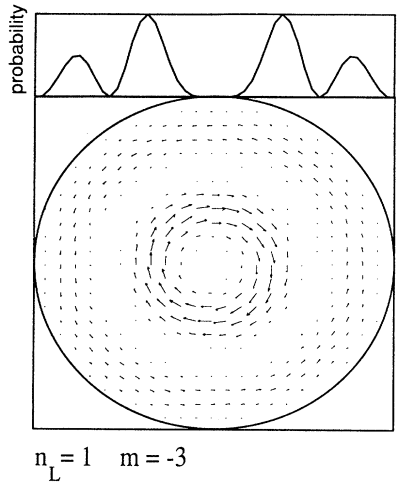

FIG. 6. Probability currents for the $n_L=1$, $m=-3$ eigenstate of a circular quantum dot. The magnetic field corresponds to $\beta=19.0$. The probability density across the dot center is shown in the upper portion of the figure.

For states with $m>0$, both $\mathbf{j}_0$ and $\mathbf{j}_A$ are positive, i.e., the current flows in the counterclockwise direction. This is the direction in which a classical electron would circulate in response to the Lorentz force from the magnetic field. For states with negative m, however, $\mathbf{j}_0$ circulates in the clockwise direction. The nonzero $\mathbf{j}_A$ is in the opposite direction and increases with radial distance r. The competition between these two terms results in the concentric rings of current moving in opposite senses as seen in Figs. 3, 5, and 6. The r dependence in (15) means that the current always flows counterclockwise at large enough r, provided the probability density has not vanished. At small values of r, the $\mathbf{j}_0$ term must always dominate and leads to the current circulating in a clockwise sense near the dot center.

If the wall boundary at the dot perimeter were not present, all the negative-m states would look similar to the condensed states—a counterclockwise circulating outer ring and a clockwise inner ring. The presence of the wall reduces the probability density near the perimeter and effectively blocks the outer ring, leaving only the clockwise inner ring. At a high enough field, the magnetic field localizes the state closer to the dot center. This "restores" the outer ring of current by moving it inward from the wall region and results in bulklike behavior. The transition between edge states and bulk states does not occur by shrinking a current ring going the "wrong" direction[14] and then reversing it as it comes near the dot center. Rather it occurs by restoring a ring of current going the "right" direction which has been suppressed by its proximity to the outer edge. The circulation going the "wrong" direction is in the center and remains there in the condensed bulklike states.

C. Connection to classical orbits

In order to make clear the correspondence between the quantum-mechanical current flows and classical orbits, let us return to the case of unbound Landau levels described by the Hamiltonian H_L [Eq. (3) above]. We can define operators X_0 and Y_0 which correspond to the classical centers of the cyclotron orbits,[15]

$$X_0=X-\frac{1}{\omega_c}V_y\ , \tag{16}$$

$$Y_0=Y+\frac{1}{\omega_c}V_x\ . \tag{17}$$

The operators V_x and V_y are defined by Eq. (1). The operator Γ^2 is then defined to be the operator corresponding to the square of the distance from the origin to the orbit center,

$$\Gamma^2=X_0^2+Y_0^2\ . \tag{18}$$

If we take the Landau-level wave functions $|n_L,m\rangle$ which are eigenvalues of L_z,

$$\Gamma^2|n_L,m\rangle=\gamma^2|n_L,m\rangle\ , \tag{19}$$

$$\gamma^2(n_L,m)=[2(n_L-m)+1]L_H^2\ , \tag{20}$$

where γ^2 is the eigenvalue of Γ^2 and $L_H=\sqrt{\hbar/eB}$ is the

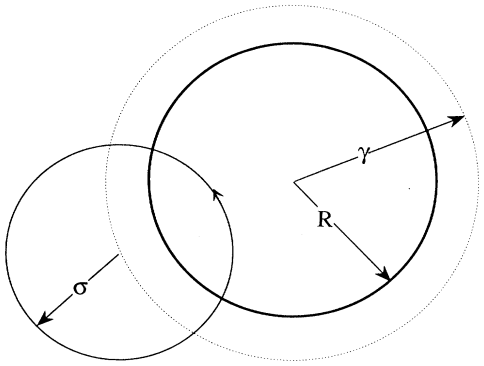

FIG. 7. The relationship between σ, the cyclotron radius, and γ, the radius of the orbit guide center. The origin is chosen to be the center of the quantum dot. The dot radius is R.

magnetic length. The classical cyclotron radius is represented by the operator

$$\Sigma^2=(X-X_0)^2+(Y-Y_0)^2 \tag{21}$$

$$=L_H^4\frac{2m^*}{\hbar^2}H_L \ , \tag{22}$$

so the eigenvalues are given by

$$\Sigma^2|n_L,m\rangle=\sigma^2|n_L,m\rangle \ , \tag{23}$$

$$\sigma^2(n_L,m)=L_H^4\frac{2m^*}{\hbar^2}(n_L+\tfrac{1}{2})\hbar\omega_c \ . \tag{24}$$

Figure 7 illustrates the relationship between γ, σ, and the origin at the dot center. The angular momentum operator L_z is related to Γ^2 and Σ^2 by

$$L_z=\frac{\hbar}{2L_H^2}(\Sigma^2-\Gamma^2) \ , \tag{25}$$

which is true classically as well.

In the unconfined Landau system, states with negative angular momentum correspond to classical orbits with centers displaced from the origin. Quantum mechanically, the position of the orbit center is not well defined since one cannot construct states which are simultaneously eigenstates of the operators X_0, Y_0, and H. The distance γ between the orbit center and the origin is a constant of the motion both classically and quantum mechanically. The cyclotron radius σ is also a good quantum number. The quantum wave function for a state with negative angular momentum corresponds, then, to all possible classical orbits of radius σ, which centers a distance γ from the origin. A circle of radius γ, centered on the origin, acts as the "guide center" for the classical orbits. As the magnetic field increases, both γ and σ become smaller. Another consequence of Eq. (20) is that states with $m=0,1,2,\ldots,n_L$ will also correspond to classical orbits with displaced orbit centers.

For the confined system, $H=H_L+V_r$, and Eqs. (20) and (24) are no longer strictly valid. For states which are already condensed and localized in the interior of the quantum dot, they will be very nearly true. We can *approximate* the value of the cyclotron radius for a particular eigenstate $|n_r,m\rangle$ of H by using Eq. (22) to define

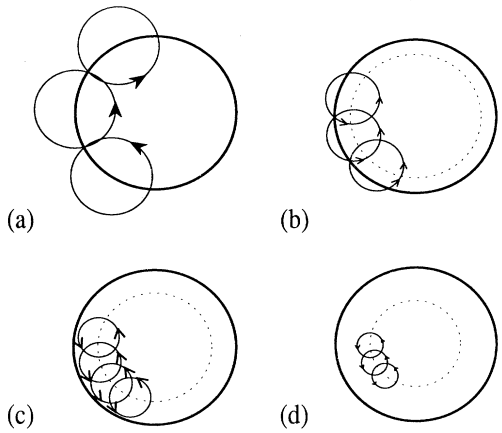

FIG. 8. Classical orbits for four increasing values of the magnetic field. The orbits (arrows), guide center (dotted), and dot wall (solid) are shown. In (a) the guide-center radius is equal to the dot radius and only a clockwise current results. As the field increases [(b)–(d)] the guide-center radius shrinks and a counterclockwise current develops around the dot perimeter, while the clockwise current becomes localized near the dot center. Orbits are chosen to correspond to specular reflection from the walls.

$$\sigma'(E)=L_H^2\sqrt{2m^*E/\hbar^2} \ , \tag{26}$$

where we use for E the *calculated* energy $E(n_r,m)$. The guide-center radius can then be obtained by using (25) to construct an approximate value,

$$\gamma'(E,m)=\sqrt{\sigma'^2(E)-2mL_H^2} \ , \tag{27}$$

where again we use the calculated value of the energy. The effect of the dot walls is then included in the raising

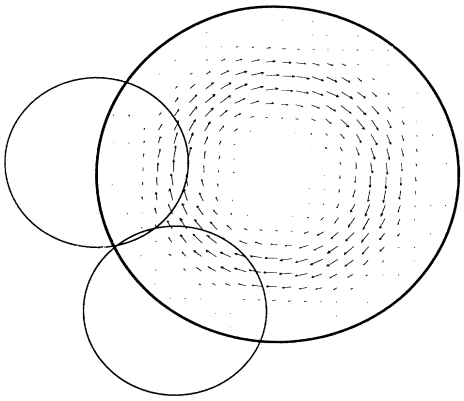

FIG. 9. Probability current for the $n_L=0$, $m=-4$ eigenstate of a circular quantum dot. The magnetic field corresponds to $\beta=11.4$ ($B=3$ T for a dot with 500-Å radius). Classical orbits calculated using Eqs. (37) and (38) are superimposed on the numerical solution.

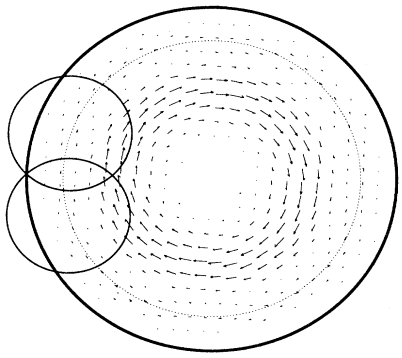

FIG. 10. Probability current for the $n_L=0$, $m=-4$ eigenstate of a circular quantum dot. The magnetic field corresponds to $\beta=15.2$ ($B=4$ T for a dot with 500-Å radius). Classical orbits calculated using Eqs. (37) and (38) are superimposed on the numerical solution.

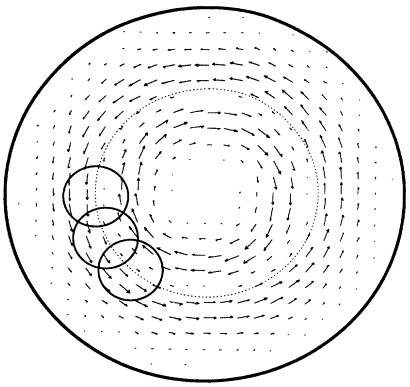

FIG. 12. Probability current for the $n_L=0$, $m=-4$ eigenstate of a circular quantum dot. The magnetic field corresponds to $\beta=30.4$ ($B=8$ T for a dot with 500-Å radius). Classical orbits calculated using Eqs. (37) and (38) are superimposed on the numerical solution.

of the eigenenergies for states which are not yet condensed in the center. Equations (26) and (27) reduce to (24) and (20) with the substitution $E=(n_L+\frac{1}{2})\hbar\omega_c$.

The classical orbits for the circular dot corresponding to quantum-mechanical eigenstates of L_z are illustrated in Fig. 8 at various stages of Landau condensation. In Fig. 8(a), the field is low and the guide-center radius $\gamma=R$. The orbits shown correspond to specular reflection off the dot walls. The current is dominantly clockwise and characteristic of a pure edge state. The guide circle (dotted) in Fig. 8(b) is inside the dot, but the orbit still corresponds to a skipping orbit, reflecting off the perimeter wall. Notice, however, that a counterclockwise current exist in the outer region between the guide circle and the dot wall. The clockwise current associated with the edge state in Fig. 8(a) has moved into the center of the dot. Figures 8(c) and 8(d) show the orbits as the magnetic field increases and the state becomes more localized and condensed. The state shown in Fig. 8(c) is not necessarily condensed, since its energy may still be elevated by proximity to the dot wall.

Figures 9–12 show the computed particle current for the $n_L=0$, $m=-4$ state at increasing magnetic fields. The values of the field are $B=3$, 4, 5, and 8 T corresponding to $\beta=11.4$, 15.2, 19.0, and 30.4. Across this range, the magnetic field transforms the state from purely edge-type, Fig. 9, to the nearly completely condensed bulk-type state shown in Fig. 12. Superimposed on the results of the Schrödinger solution are the classical orbits calculated using Eqs. (26) and (27). The relation between the classical current flows due to the orbits and the quantum results verifies the explanation above and demonstrates the utility of the quantities σ' and γ' in describing the confined states. Orbits computed using the unconfined 2DEG values σ and γ yield a much worse comparison with the calculated current patterns.

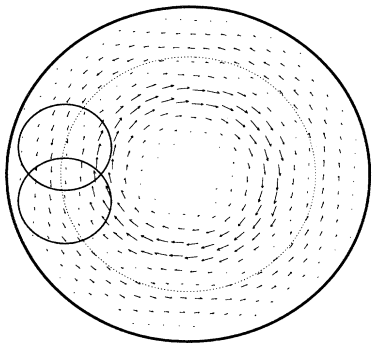

FIG. 11. Probability current for the $n_L=0$, $m=-4$ eigenstate of a circular quantum dot. The magnetic field corresponds to $\beta=19.0$ ($B=5$ T for a dot with 500-Å radius). Classical orbits calculating using Eqs. (37) and (38) are superimposed on the numerical solution.

IV. SOFT BOUNDARIES

Actual quantum dots or wires would not have abrupt hard-wall boundaries. The confining potential would be the result of the self-consistent solution of the Poisson equation for the band bending inside the semiconductor.

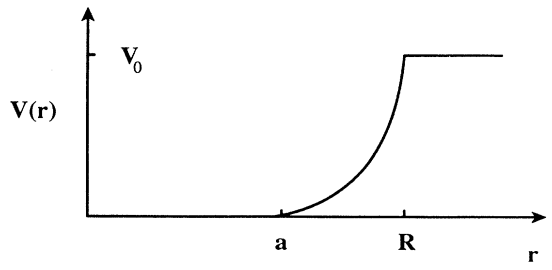

FIG. 13. Radial potential profile of quantum dot with parabolic walls.

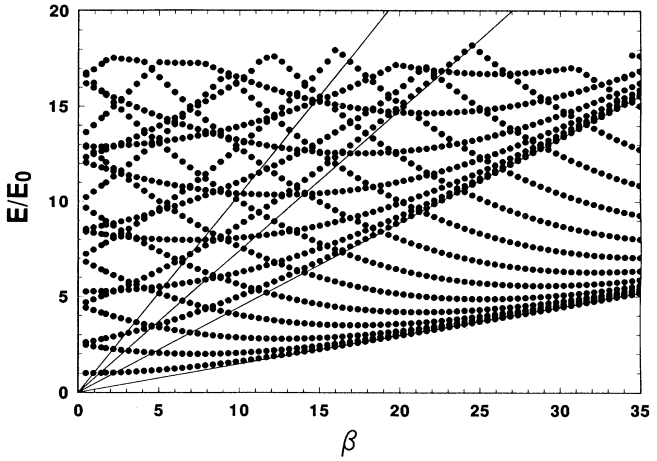

FIG. 14. Bound-state energy levels of a circular quantum dot with parabolic walls as a function of applied magnetic field. The radial potential profile is as depicted in Fig. 13 with $a=400$ Å, $R=500$ Å, and $V_0=200$ meV. $\beta=eB\pi R^2/\pi\hbar$ is a dimensionless measure of the magnetic field strength. The energies are in units of E_0, the zero-field ground-state energy.

Several calculations have shown that this potential can often be approximated by a flat ($V=0$) region and parabolically increasing walls.[8,16,17] We are particularly interested in eventually making a connection to the experiments of Reed *et al.*, after whose potential profiles we have roughly modeled ours. The effects of soft walls on the energy levels is considered here by calculating the eigenstates for a confined quantum dot with such a potential profile, as shown in Fig. 13. The radius of the inner, flat region is a, the outer radius is R, and the value of the potential at the outer rim ($r=R$) is V_0. In both of the cases examined here $R=500$ Å, $V_0=200$ meV. Figure 14 shows the energy levels as a function of applied magnetic field for $a=400$ Å. Figure 15 shows the results for $a=250$ Å. Clearly the primary effect of the walls coming in closer toward the center is to inhibit condensation until the wave functions are confined by the magnetic field to the central flat region. The qualitative discussion of the transformation of the states into Landau levels remains unchanged.

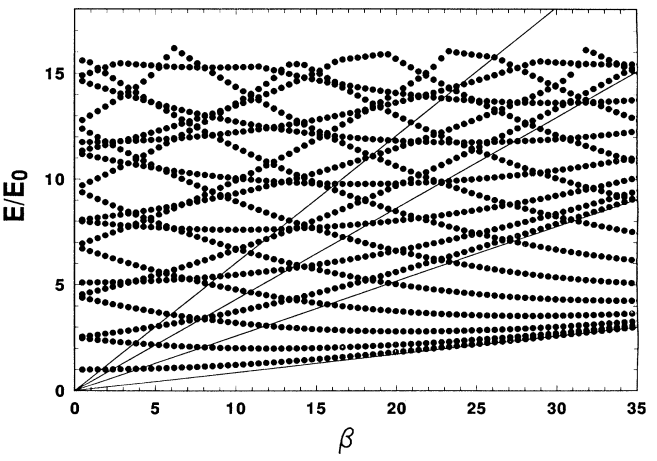

FIG. 15. Bound-state energy levels of a circular quantum dot with parabolic walls as a function of applied magnetic field. The radial potential profile is as depicted in Fig. 13 with $a=250$ Å, $R=500$ Å, and $V_0=200$ meV. $\beta=eB\pi R^2/\pi\hbar$ is a dimensionless measure of the magnetic field strength. The energies are in units of E_0, the zero-field ground-state energy.

V. CONCLUSION

In an unconfined 2DEG the degenerate Landau levels can be decomposed into eigenstates of angular momentum. States with negative angular momentum produce current distributions consisting of concentric rings with counter-circulating flows. The negative angular momentum states can be identified with classical orbits with orbit centers displaced from the origin. This identification was made by Darwin in his seminal paper, in which he examined states in a parbolic confining potential. In *that* context, he also correctly identified the negative-m states with edge states. In a parabolic potential Landau condensation never really occurs—the states always feel the effects of the potential.

In the hard-wall circular dot, negative-m states are pure edge states only at low magnetic fields. They are characterized by a single clockwise current flow near the dot perimeter. As the field increases, a counterclockwise current appears at the perimeter and the clockwise flow is squeezed inward. In this intermediate regime, the clockwise "skipping" current is not an edge current but rather a *central* current. At high fields both rings of opposing current are localized in the central region of the dot and the state becomes similar (asymptotically) to bulk Landau levels.

Numerical solutions of the Schrödinger equation for an electron in a quantum dot have been performed and the particle currents associated with particular eigenstates analyzed. The correspondence between the quantum current flows and the classical orbits has been established using approximate expressions for the guide-center radius and cyclotron radius which include the effect of the confining potential walls. The effects of softer, parabolic walls have been examined.

Note added in proof After completion of this work, I received a copy of work by Geerinckx, Peeters, and Devreese,[18] related to the effect of soft boundaries as discussed in Sec. IV.

ACKNOWLEDGMENTS

The author wishes to thank Wolfgang Porod for helpful discussions and Steven E. Laux for a copy of his calculation prior to publication. This work was supported by the Air Force Office of Scientific Research and by the National Science Foundation under Grant No. ECS890025 through the National Center for Computational Electronics and utilized the Cray-2 at the National Center for Supercomputing Applications, University of Illinois at Urbana-Champaign.

[1]C. G. Darwin, Proc. Cambridge Philos. Soc. **27**, 86 (1930).
[2]R. B. Dingle, Proc. R. Soc. London, Ser. A **212**, 47 (1952); **219**, 463 (1953).
[3]Marko Robnik, J. Phys. A **19**, 3619 (1986).
[4]W. Hansen, T. P. Smith, J. A. Brum, J. M. Hong, K. Y. Lee, C. M. Knoedler, D. P. Kern, and L. L. Chang, in *Nanostructure Physics and Fabrication,* edited by M. A. Reed and W. P. Kirk (Academic, Boston, 1989).
[5]M. Reed, J. Randall, J. Luscombe, W. Frensley, R. Aggarwal, R. Matyi, T. Moore, and A. Wetsel, Festkorperprobleme **29**, 267 (1989).
[6]A. Lorke, J. P. Kotthaus, and K. Ploog, Phys. Rev. Lett. **64**, 2559 (1990).
[7]C. T. Liu, K. Nakamura, D. C. Tsui, K. Ismail, D. A. Antoniades, and H. I. Smith, Appl. Phys. Lett. **55**, 168 (1989).
[8]Arvind Kumar, Steven E. Laux, and Frank Stern, Phys. Rev. B **42**, 5166 (1990).
[9]P. A. Maksym, and Tapash Chakraborty, Phys. Rev. Lett. **65**, 108 (1990).
[10]H. Stikova, L. Smrcka, and A. Isihara, J. Phys. Condensed Matter **1**, 7965 (1989).
[11]J. F. Weisz and K.-F. Berggren, Phys. Rev. B **41**, 1687 (1990).
[12]Ch. Sikorski and U. Merkt, Phys. Rev. Lett. **62**, 2164 (1989).
[13]T. Demel, D. Heitmann, P. Grambow, and K. Ploog, Phys. Rev. Lett. **64**, 788 (1990).
[14]The "wrong" circulation here means opposite that of a classical circular cyclotron orbit centered at the dot center.
[15]C. Cohen-Tannoudji, B. Diu, and F. Laloë, *Quantum Mechanics* (Wiley, New York, 1977), p. 742.
[16]K.-F. Berggren, T. J. Thornton, D. J. Newson, and M. Pepper, Phys. Rev. Lett. **57**, 1769 (1986).
[17]J. F. Weisz and K.-F. Berggren, Phys. Rev. B **40**, 1325 (1989).
[18]F. Geerinckx, F. M. Peeters, and J. T. Devreese, J. Appl. Phys. **68**, 3435 (1990).